Geomechanics and Engineering, *Vol. 41, No. 2 (2025) 221-232*
https://doi.org/10.12989/gae.2025.41.2.221

Investigating rutting performance of unpaved roads with recycled concrete aggregates using small-scale cyclic loading tests

Jiacheng Qiu[a], Yuekai Xie[b], Yue Chen*, Ben Reissenweber[c], Chen Wang[d], Ziheng Wang[e] and Jianfeng Xue[f]

School of Engineering and Technology, The University of New South Wales, Canberra, Australia

(*Received Novemeber 18, 2024, Revised March 20, 2025, Accepted April 3, 2025*)

Abstract. The recycling and reuse of construction and demolition materials offer significant environmental and economic benefits. This study investigated the performance of aggregates with varying proportions of recycled concrete aggregate (RCA) and natural aggregate (NA) as base materials. Key parameters, such as compaction behaviour, California bearing ratio (CBR), and resilient modulus, were evaluated. The findings revealed that the mixture with 50% RCA and 50% NA exhibited the highest CBR and resilient modulus values. Small-scale cyclic loading tests were then conducted on the samples of NA, RCA, and a 50% RCA-50% NA mixture to assess the suitability of RCA as a base material. Additionally, RCA and NA samples were reinforced with biaxial geogrids for material optimisation. The results showed that the 50% RCA-50% NA mixture exhibited the smallest permanent deformation, and the geogrid, placed at the middle depth of the base, significantly reduced rut depth. Findings of this experimental study suggest that RCA can be used as an alternative base material to partially replace NA in road construction. The results can help conserve natural resources, promote sustainability through the reuse of waste materials, and reduce the environmental impact associated with the use of NA in road construction.

Keywords: geosynthetics; granular materials; ground improvement; reinforced soil; road engineering

1. Introduction

The rapid increase in urbanisation has resulted in the expansion of transportation infrastructure over the past few decades. Natural aggregate (NA), primarily composed of crushed stone, gravel, and sand, serves as a key component in pavement construction. As reported by Van Dam *et al.* (2015), aggregates make up 80 to 85% of the total volume in rigid (concrete) pavements and 62 to 68% of the total volume in flexible pavements. Consequently, large quantities of NAs have been consumed in pavement construction, raising concerns about the depletion of natural aggregate sources and the environmental impacts associated with their extraction and transportation. In addition, a large amount of construction and demolition (C&D) waste is generated globally every year. According to the latest National Waste Report (NWR 2022), approximately 25.2 Mt of C&D waste was produced in 2020-21. As stated in the report, approximately 80% of C&D waste was recycled for use as road base or aggregates, which is promising. However, 20% of C&D waste was still disposed of in landfills, resulting not only in environmental concerns but also in the consumption of finite land resources. As a result, there is growing interest in developing sustainable methods for reusing C&D waste materials in construction, particularly through the use of recycled concrete aggregate (RCA).

RCA, produced by crushing and processing waste concrete, has gained attention as a potential substitute for NA in various civil engineering applications, including road construction (Nam *et al.* 2023, Ok *et al.* 2023). Previous research has extensively investigated the engineering properties of RCA, such as its grading, strength, LA abrasion, durability, and California bearing ratio (CBR) (Arulrajah *et al.* 2012, Gabr and Cameron 2012, Arulrajah *et al.* 2014, Toka and Olgun 2022). Numerous studies have reported that RCA exhibits mechanical properties comparable to those of NA, making it a suitable alternative for use in road base and subbase layers. The successful incorporation of RCA in road construction provides a sustainable solution for C&D waste management while also reducing the demand for virgin natural aggregates, thereby mitigating the environmental impact of aggregate mining. VicRoads (2011) permits the use of RCA material as pavement subbase and light-duty base works, subject to some requirements. However, in order to maximise the usage of RCA, its mechanical properties need to be further explored to assess its suitability as a base material in pavements.

Repeated load triaxial test (RLTT) has been widely adopted by many researchers to investigate the mechanical properties of RCA (Arm 2001, Gabr and Cameron 2012, Azam and Cameron 2013, Gabr *et al.* 2013, Alnedawi and

*Corresponding author, Ph.D.
E-mail: yue.chen4@unsw.edu.au
[a]Ph.D. Student
[b]Ph.D.
[c]Bachelor Student
[d]Bachelor Student
[e]Ph.D. Student
[f]Ph.D.

ISSN: 2005-307X (Print), 2092-6219 (Online)

Rahman 2021, Wang *et al.* 2023). Gabr and Cameron (2012) reported that the resilient moduli of RCA are greater, and the permanent strains are lower, compared to those of NA based on the results of RLTTs. Azam and Cameron (2013) conducted RLTTs on NA and RCA specimens with different moisture contents and concluded that both the resilient modulus and permanent strain are affected by the moisture content level. An increase in moisture content results in a decrease in resilient modulus and an increase in permanent strain. Wang *et al*. (2023) reported that the resilient behaviour of RCA is similar to that of NA. However, the RLTT results also indicated that RCA with low parent concrete strength and high amounts of rounded particles can result in poor pavement performance and should be limited in pavement construction. In general, most studies have concluded that the mechanical properties of RCA are comparable to those of NA and that RCA can be used in pavements. However, there remains a significant gap in understanding the effects of subgrade conditions on overall pavement performance when RCA is used as a base material.

The subgrade, serves as the foundation of the pavement structure, plays a crucial role in determining the overall performance and stability of the pavement. Since a weak subgrade cannot provide the same level of support to the base layer as a strong subgrade, it can influence load distribution and cause increased deformation within the pavement. In addition, subgrades with low strength, typically those with CBR values below 3%, are common in many regions worldwide, including Australia. The presence of weak subgrades often results in excessive deformations under traffic loads, which significantly reduces the serviceability of roads and increases maintenance costs. However, few studies have examined the impact of the subgrade on the behaviour and suitability of RCA in pavements. To mitigate the effects of weak subgrades, thicker base layers with high-quality aggregates are often required to provide adequate support for traffic loads (Al-Swaidani *et al.* 2024). Therefore, to obtain a comprehensive understanding of the suitability of RCA as a base material, it is essential to evaluate its performance in pavements constructed over low-strength subgrades, assessing whether it can provide a sustainable and durable alternative to NA under these challenging conditions.

This paper aims to investigate the suitability of partially or completely replacing NA with RCA as base material over weak subgrades in unpaved roads through a series of small-scale cyclic loading tests. Tests were conducted with three types of base materials, namely NA, RCA, and a mixture of both NA and RCA. To ensure a direct comparison, the grading of RCA was modified to align with that of NA. Surface displacements were measured during the tests to evaluate the performance of each base material. To maximise the adoption of RCA, a geogrid was incorporated to enhance its strength and extend its service life. The findings of this study provide valuable insights into the effectiveness of RCA as a base material over weak subgrades. Additionally, the results contribute to the conservation of natural resources, promote sustainability through the reuse of waste materials, and reduce the environmental impact associated with the use of NA in road construction.

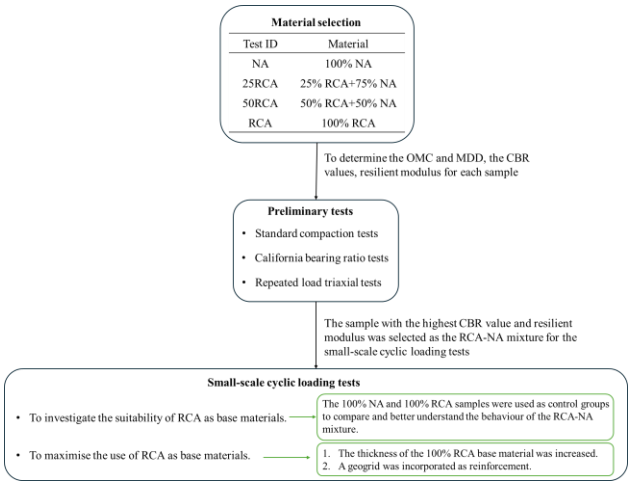

Fig. 1 Flowchart of the experimental plan

2. Materials and methods

This paper presents a laboratory investigation aimed at assessing the suitability of partially or fully replacing NA with RCA as a base material in pavements. Fig. 1 presents the flowchart of the experimental plan. In this study, RCA was mixed with NA at various percentages, and preliminary tests, including standard compaction tests, California bearing ratio tests, and RLTTs, were conducted to determine the optimum moisture content (OMC) and maximum dry density (MDD) of these mixtures. The determined OMC and MDD were then used to prepare samples for CBR tests and RLTTs. The RCA and NA mixture with the highest CBR value and resilient modulus was selected for small-scale cyclic loading tests. Additionally, 100% NA and 100% RCA samples were tested as control groups to compare and enhance the understanding of RCA and NA mixture behaviour. In the small-scale cyclic loading tests, the effects of increasing the RCA layer thickness and using a geogrid as reinforcement were studied to maximise the use of RCA in the base layer.

2.1 Materials

2.1.1 Base material

Two types of base materials were adopted in this study, namely NA and RCA. NA served as the control group to compare its properties with those of RCA. The NA is a commercially supplied crushed Blue Metal, as shown in Fig. 2(a), and its particle size distribution is presented in Fig. 3. According to the Unified Soil Classification System (USCS), NA is classified as well-graded gravel (GW).

The RCA used in this study was sourced from ACT Recycling in Canberra, Australia, as shown in Fig. 2(b). The particle size distribution of RCA is displayed in Fig. 3. To facilitate a direct comparison between RCA and NA, the RCA was sieved to match the particle size distribution of NA. The particle size distribution of the sieved RCA is also included in Fig. 3. It can be seen that the sieved RCA

(a) NA (b) RCA

(c) Black clay

Fig. 2 Photos of materials used in this study

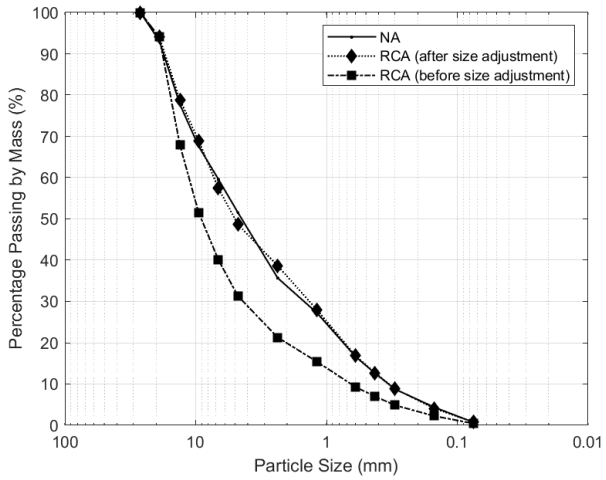

Fig. 3 Particle size distribution of NA and RCA before and after size adjustment

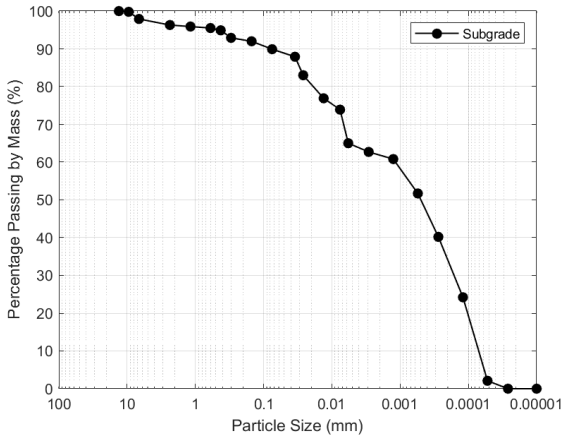

Fig. 4 Particle size distribution of subgrade

exhibits a similar particle size distribution to that of NA. In this study, RCA and NA were mixed in weight ratios of 0:1 (0% RCA), 1:3 (25% RCA), 1:1 (50% RCA), and 1:0 (100% RCA). Standard compaction tests, CBR tests, and RLTTs were conducted on these mixtures. Based on the results of CBR tests and RLTTs, the mixture with the highest CBR and resilient modulus was selected as the base material for small-scale cyclic loading tests. The setup of small-scale cyclic loading tests is detailed in the following sections.

2.1.2 Subgrade material

The subgrade material used in this study is black clay, as shown in Fig. 2(c). The particle size distribution of the subgrade soil is presented in Figure 4. Based on the USCS, this soil is classified as high plastic silt (MH). A series of tests were conducted to determine the properties of subgrade soil as per ASTM guidelines (ASTM-D4318, 2018, ASTM-D698, 2021, ASTM-D1883, 2021), and the determined properties are summarised in Table 1.

Table 1 Properties of subgrade materials used in this study

Properties	Subgrade
Plastic limit	43%
Liquid limit	84%
Plasticity Index	41%
USCS	MH
OMC	32.4%
MDD	1,290 kg/m^3
CBR at OMC and MDD	10% (Unsoaked)

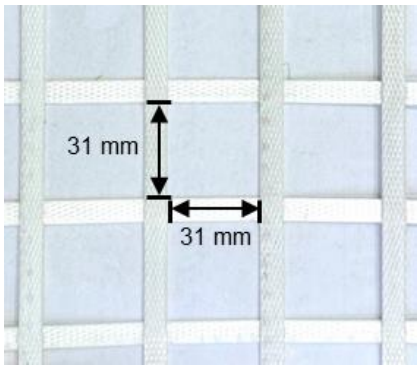

Fig. 5 GG40 used in this study

Table 2 Properties of geogrids

Properties	Units	Biaxial GG40
Aperture size	mm	31
Tensile strength at 2% elongation	kN/m	16
Tensile strength at 5% elongation	kN/m	32
Ultimate tensile strength	kN/m	≥ 40
Elongation at ultimate strength	%	≤ 7

As shown in Table 1, the CBR of the subgrade soil at its MDD with OMC is approximately 10%. To assess the suitability of RCA as a base material under worst field conditions, the CBR of the subgrade soil was reduced to simulate a weak subgrade layer. Therefore, a series of unsoaked CBR tests were performed, with the subgrade soil prepared at varying moisture contents and dry densities to achieve a CBR value of less than 3%. In this study, the subgrade soil was prepared with a moisture content of 46.6% at 91.5% of the MDD, resulting in a CBR value of 2.7%.

2.1.3 Geogrids

The geosynthetic employed in this study is a biaxial geogrid, GG40, as shown in Fig. 5. Table 2 summarises the geogrid properties as provided by the manufacturer. This geogrid exhibits identical properties in both the machine and cross-machine directions, with an ultimate tensile strength exceeding 40 kN/m in both directions.

2.2 Preliminary tests

2.2.1 Standard compaction tests

Compaction tests were conducted on RCA-NA mixtures with moisture contents varying from 6 to 12%, with standard compaction effort defined in ASTM D698 (ASTM-D698, 2021). Sam ples with different moisture contents were compacted in 3 layers with 25 blows per layer in the standard compaction mould. The moisture content was measured from the materials before compaction as moisture can be partially drained during compaction.

2.2.2 California bearing ratio test

The CBR tests were performed on RCA-NA mixtures. The standard CBR mould, with a diameter of 152.4 mm and a height of 125 mm, along with a 50 mm diameter loading plunger, was used in the tests. All test samples were prepared at the OMC and MDD under the standard compaction effort. After preparation, the unsoaked CBR values of RCA-NA mixture were determined under the loading rate of 1.25 mm/min.

Table 3 The loading sequences used in the RLT tests

Confining pressure (kPa)	Stage	Deviator stress (kPa)
30	1	15
	2	30
	3	60
	4	120
60	1	30
	2	60
	3	120
	4	240

2.2.3 Repeated load triaxial test

The resilient modulus (Mr) of RCA-NA mixture was determined using RLTTs. The samples were prepared in a split mould with a diameter of 100 mm and the height of 200 mm at corresponding OMC and MDD using the standard compaction energy. A haversine-shaped wave loading pulse was adopted with a loading period of 0.1 s and the resting period of 0.9 s, as per AASHTO T307 guidelines (AASHTO 2017). To ensure the stability of the sample, 10% of the applied deviator stress was used as the resting load. A pre-loading stage of 1,000 cycles was conducted for each sample with a confining pressure of 30 kPa and a deviator stress of 60 kPa. Two confining pressures, namely 30 and 60 kPa, were adopted to assess the effects of confining pressure on the behaviour of RCA. Table 3 shows the deviator stresses and confining pressures used in the RLTTs, with each stage consisting of 300 cycles. For each test, at least two samples were prepared to ensure the repeatability of the test results.

2.3 Small-scale cyclic loading test

2.3.1 Testing mould

To investigate the impact of traffic loads on pavement performance, a series of cyclic loading tests was conducted using a small-scale testing mould. This mould consists of a circular base plate and a cylindrical plastic wall, as shown in Fig. 6. The cylindrical mould has an inner diameter of 390 mm and a height of 620 mm, with a wall thickness of 30 mm. The dimensions of the mould were carefully measured before and after each test to ensure there was no deformation of the mould. The circular base plate is constructed from an aluminium plate with a diameter of 520 mm and a thickness of 50 mm. The cylindrical wall and the base plate are secured together using eight bolts through pre-drilled holes.

A circular steel top plate, fabricated to fit onto the cylindrical wall, has a diameter of 520 mm and includes a central 60 mm diameter circular hole to allow the loading plunger to pass through. Similar to the base plate, the top

Fig. 6 Testing mould

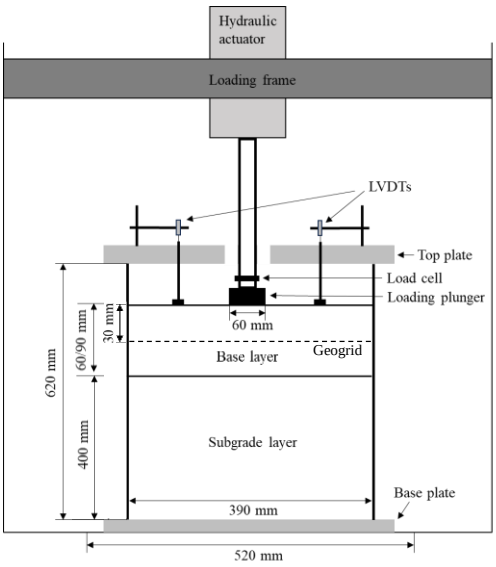

Fig. 7 Schematic diagram of the test setup

plate is also attached to the cylindrical wall using eight bolts through pre-drilled threaded holes, after the sample has been prepared. To facilitate surface displacement measurements, four steel rods with small metal plates at one end are constructed. The metal plates are placed on the surface of the base layer, while four diametrically opposite holes, drilled in the top plate at a distance of 100 mm from the centre of the loading plunger, allow the rods to pass through. Four linear variable differential transducers (LVDTs) are then positioned to measure the vertical displacements of the rods, as shown in Fig. 7.

The load is applied through the loading plunger, which is attached to a hydraulic actuator with a maximum capacity of 500 kN. The loading plunger has a diameter of 60 mm, approximately 1/6.5 of the mould diameter (390 mm), a ratio recommended by Abu-Farsakh *et al.* (2016) to effectively minimise boundary effects. The vertical displacements of the loading plunger, which reflect the vertical displacements at the centre of the top base layer, are measured directly by the hydraulic actuator. Fig. 7 shows a schematic diagram of the test setup.

2.3.2 Sample preparation

The subgrade soil was air-dried and crushed. Then the NA, RCA, and subgrade soil were oven-dried separately for at least 24 hours. The RCA-NA mixture was then prepared by combining the oven-dried RCA and NA in the corresponding ratio by weight. The NA, RCA, and RCA-NA mixture were each mixed with water to achieve their respective OMCs, as determined from the standard compaction tests. The subgrade soil was mixed with water to achieve a moisture content of 46.6%, as specified in Section 2.1.2, and then stored in airtight containers for at least 24 hours to ensure uniform water distribution.

In this study, the thickness of subgrade was 400 mm, and the base layer thickness was selected as either 60 or 90 mm to maintain a 1:1 or 1:1.5 ratio with the loading plunger diameter. According to Chummar (1972) and Lee and Salgado (2005), the influence depth of a circular footing approximately equates to the footing diameter, D. In addition, based on Boussinesq's stress theory (Boussinesq and Caquot 1885), the vertical stress beneath the centre of a uniformly loaded circular footing decreases to approximately 28% of the applied surface vertical stress at a depth of 1D, and further reduces to about 14% at 1.5D. Beyond this depth, the stress increase induced by the footing becomes negligible. Therefore, with a further increase in base thickness, its influence on overall pavement performance would also be negligible.

The subgrade was compacted in the testing mould in eight layers to a dry density of 1,180 kg/m^3, which was 91.5% of the MDD. Each subgrade layer was compacted to a thickness of 50 mm using a 2.5 kg hammer with manual compaction. To improve bonding between successive layers, the surface of each compacted subgrade layer was manually scratched before placing the next layer. The base course was prepared by compacting the aggregates in 30 mm layers using a demolition hammer. The weight of base materials used for each layer was carefully measured, and a 30 mm reference line was marked on the side of the mould to ensure consistent layer thickness. Additionally, the compaction pattern was consistently followed for each layer. Approximately 10 mins were used to prepare each base layer. For samples with a 60 mm base layer, the geogrid was placed at the mid-depth of the base layer. The geogrid was cut into a 390 mm diameter circle to align with the testing mould diameter. After preparing the first 30 mm of the base layer, the geogrid was placed on its surface, and the second 30 mm layer was then constructed following the procedures mentioned above. To ensure test consistency, all samples were prepared under controlled laboratory conditions, using the same preparation methods and duration.

2.3.3 Test procedure

To evaluate the performance of NA, RCA and the RCA-NA mixture under various applied stresses, a multi-stage cyclic loading test was conducted. This approach provides a fundamental understanding of the behaviour of different materials under a range of loading conditions with the minimum number of tests required. As shown in Fig. 8(a), five stress amplitudes were used: 150 (stage 1), 250 (stage

Table 4 Small-scale cyclic loading test program

Test ID	Base material	Base thickness (mm)	Reinforcement condition
NA	100% NA	60	Unreinforced
RCA	100% RCA	60	
RCA 90	100% RCA	90	
RCA-NA mixture	RCA and NA mixed by weights	60	
Reinforced NA	100% NA	60	GG40
Reinforced RCA	100% RCA	60	

2), 350 (stage 3), 450 (stage 4), and 550 kPa (stage 5), with 10,000 cycles performed at each of the first four stress levels and 50,000 cycles conducted at the 550 kPa loading amplitude. The 550 kPa amplitude simulates the standard tyre pressure corresponding to a standard axle load of 80 kN, therefore, a greater number of loading cycles was applied at this amplitude to investigate the long-term performance and suitability of RCA as a base material for unpaved roads. The loading frequency of 0.77 Hz was adopted, with a 0.8 s of loading period and a 0.5 s resting period, as shown in Fig. 8(b).

Table 4 summarises the test program for the small-scale cyclic loading tests used in this study. The 100% NA and 100% RCA were used as control groups to compare and understand the behaviour of the RCA-NA mixture. The weight ratio for the RCA-NA mixture was determined based on the results of CBR tests and RLTTs, as details in Sections 3.1.2 and 3.1.3.

3. Results and discussion

3.1 Preliminary test results

3.1.1 Compaction test results

The OMC and MDD of RCA-NA mixtures obtained from standard compaction tests, are shown in Table 5. The OMC of RCA is greater than that of NA, which can be attributed to the higher water absorption capacity of RCA compared to NA (Gómez-Soberón 2002, Katz 2003, Xiao *et al*. 2005). Therefore, the OMC of RCA-NA mixtures increases with RCA content, ranging from 8% at 0% RCA to 10.2% at 100% RCA. The MDD of the mixture decreases with increasing RCA content, with the 100% NA sample having the highest MDD and the 100% RCA sample the lowest. This is due to the residual cement mortar attached to the RCA, which has a lower density (Sagoe-Crentsil *et al*. 2001).

3.1.2 CBR test results

The CBR values for RCA-NA mixtures are summarised in Table 5. It can be seen that the 100% NA and the 100% RCA samples have comparable CBR values, with 100% RCA has a slightly higher CBR value. This can be attributed to the greater intrinsic strength of RCA, which results from the cementitious particles in RCA that improve

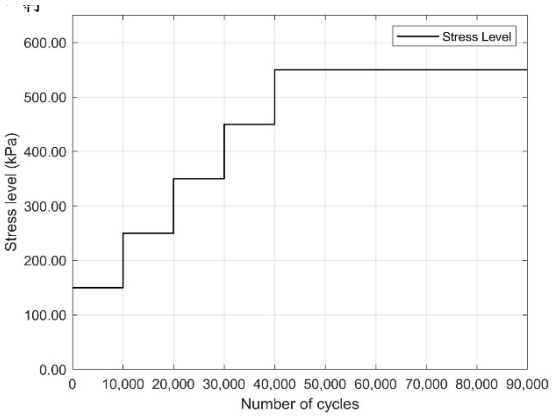

(a) loading stages

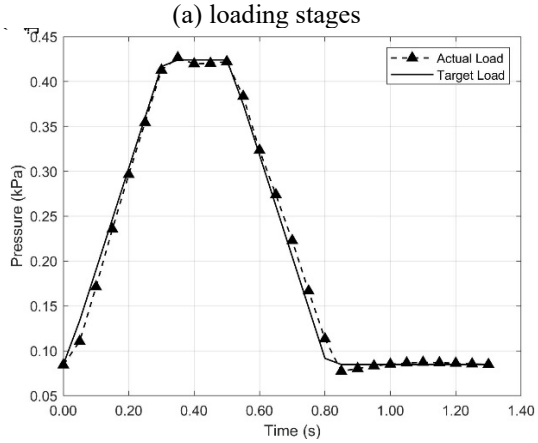

(b) loading waveform

Fig. 8 Multistage loading test program for small-scale cyclic loading tests

Table 5 Results of compaction and CBR tests for the RCA-NA mixtures

RCA content (%)	NA content (%)	OMC (%)	MDD (kg/m^3)	CBR (%)
0	100	8.0	2,090	65.0
25	75	9.2	2,040	68.1
50	50	9.8	1,980	71.1
100	0	10.2	1,850	66.6

the bonding between aggregates. Additionally, it can be observed that the RCA-NA mixtures have greater CBR values compared to the 100% RCA sample, with the mixture of 50% RCA and 50% NA having the highest CBR. This may be attributed to the lower density and higher moisture content of the RCA, which reduce its load-bearing capacity (Thai *et al.* 2022). All samples have CBR values greater than 60%, which can be classified as Type 2.2 materials according to Transport and Main Roads Specifications (2022), making them suitable for use as base or subbase materials in pavements.

3.1.3 Resilient modulus

The Mr of the RCA-NA mixture was calculated at the end of each loading stage in the RLTTs, and the results are presented in Fig. 9. In general, the resilient modulus of all samples increases with the deviator stress, regardless of

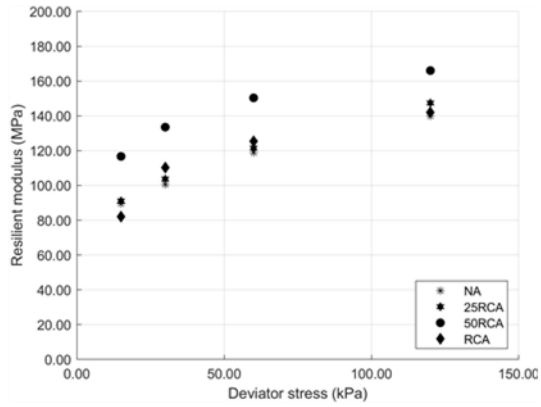

(a) 30 kPa confining pressure

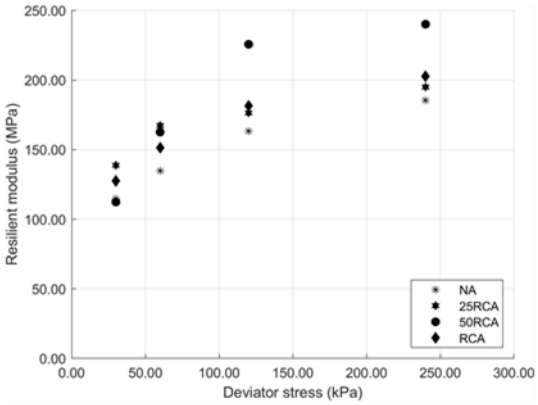

(b) 60 kPa confining pressure

Fig. 9 Resilient moduli of RCA-NA mixtures measured under: (a) 30 kPa confining pressure and (b) 60 kPa confining pressure

RCA content or applied confining pressure. This is because higher deviator stress enhances the strength of the samples, resulting in smaller elastic deformations (Gu *et al*. 2015). Applying greater confining pressure to the samples also increases the resilient modulus due to the improved strength. It can be observed that under a given confining pressure and deviator stress, the resilient modulus of RCA is slightly greater than that of NA, and the RCA-NA mixture with a 1:1 weight ratio (50% RCA and 50% NA) exhibits the highest resilient modulus in most conditions. Since the 50% RCA and 50% NA mixture, referred to as 50RCA-50NA in the following context, demonstrated the greatest CBR value and resilient modulus, it was selected as the base material for use in the small-scale cyclic loading tests.

3.2 Small-scale cyclic loading test results

3.2.1 Effects of RCA on rutting performance

As mentioned above, the 50RCA-50NA sample exhibited the highest CBR value and resilient modulus. Therefore, in the small-scale cyclic loading tests, NA (100% NA), RCA (100% RCA), and 50RCA-50NA were used as base materials to study the effects of RCA on rutting performance.

Fig. 10 illustrates the development of cumulative permanent surface displacements with the number of cycles, measured at the centre of the loading plunger for samples constructed with these three materials in a 60 mm-thick base layer. Results show that the permanent deformation increases with the number of load cycles. The permanent deformation increases significantly during the first few loading cycles at each loading stage, after which the rate of rutting depth increase reduces as the number of cycles continues to increase. The test with 100%NA base material failed after approximately 30,000 cycles, with an accumulated permanent deformation of 10.4 mm. However, specimens with RCA and the 50RCA-50NA mixture exhibit significant rutting resistance, with the 50RCA-50NA mixture showing the smallest rut depth. Both RCA and the 50RCA-50NA mixture have higher CBR values than NA, indicating greater intrinsic strength. Additionally, both RCA and the 50RCA-50NA mixture have higher OMCs than NA. This can be attributed to the residual cement mortar in the RCA and the crushing process undergone by the RCA, which increases its water absorption capacity compared to NA (Gómez-Soberón 2002, Katz 2003, Xiao *et al.* 2005). Furthermore, RCA exhibits a greater OMC and lower MDD than the 50RCA-50NA mixture, resulting in a higher water content in the small-scale cyclic loading test samples. During cyclic loading, greater fluctuations in pore water pressure reduce the rutting resistance of the RCA specimens. Consequently, the 50RCA-50NA mixture demonstrates the smallest displacement among these three base materials.

3.2.2 Effects of base thickness on rutting performance

Fig. 11 shows the effects of base thickness on the permanent deformation of RCA. As one would expect, increasing the base layer thickness from 60 mm to 90 mm reduced the permanent deformation from 10.2 mm to 6.2 mm by the end of the test. According to Boussinesq's stress distribution theory, the vertical stress beneath a circular footing decreases from approximately 28% of the applied surface stress at a depth of 1D to around 14% at a depth of 1.5D. Therefore, as the thickness of the base layer increases, the vertical stress applied to the subgrade decreases, resulting in a reduction in rutting depth. However, the 90 mm-thick RCA base still exhibits a greater rut depth compared to that of the 50RCA-50NA mixture. To optimise the use of waste materials, further efforts are required to reduce the rut depth of the RCA sample.

3.2.3 Effects of geogrid on rutting performance

The geogrid was placed at the mid-depth of the 60 mm thick base layer in both the NA and RCA samples to optimise material performance by enhancing their rutting resistance.

As shown in Fig. 12, both reinforced NA and reinforced RCA exhibit lower permanent deformations than unreinforced samples, demonstrating the effectiveness of reinforcement in reducing deformation under loading. When comparing the rut depth of the geogrid-reinforced NA sample to the unreinforced NA sample, it is clear that the inclusion of the geogrid significantly extends the service life of the NA sample, which previously failed after

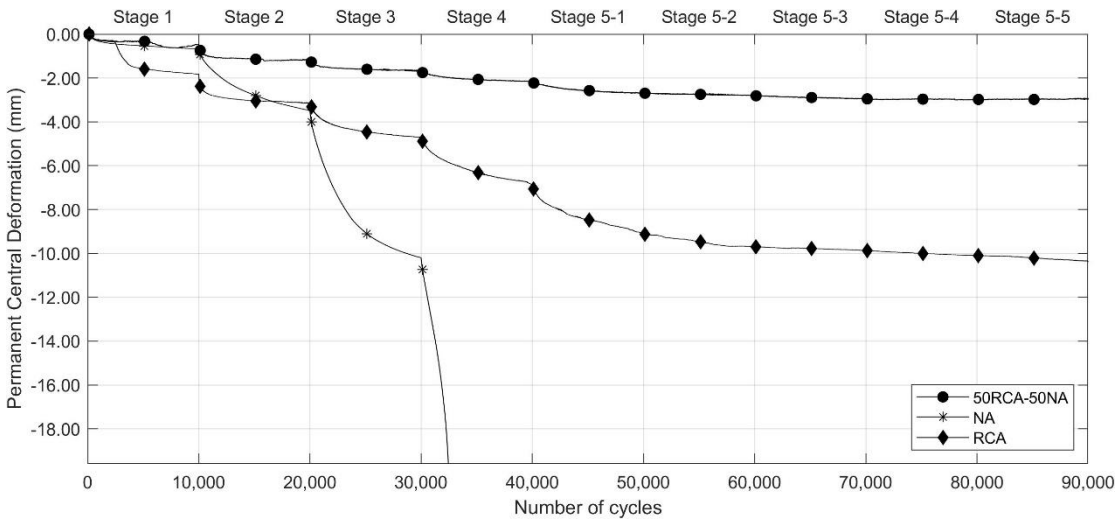

Fig. 10 Surface displacements for NA, RCA, and 50RCA-50NA samples with a 60 mm base

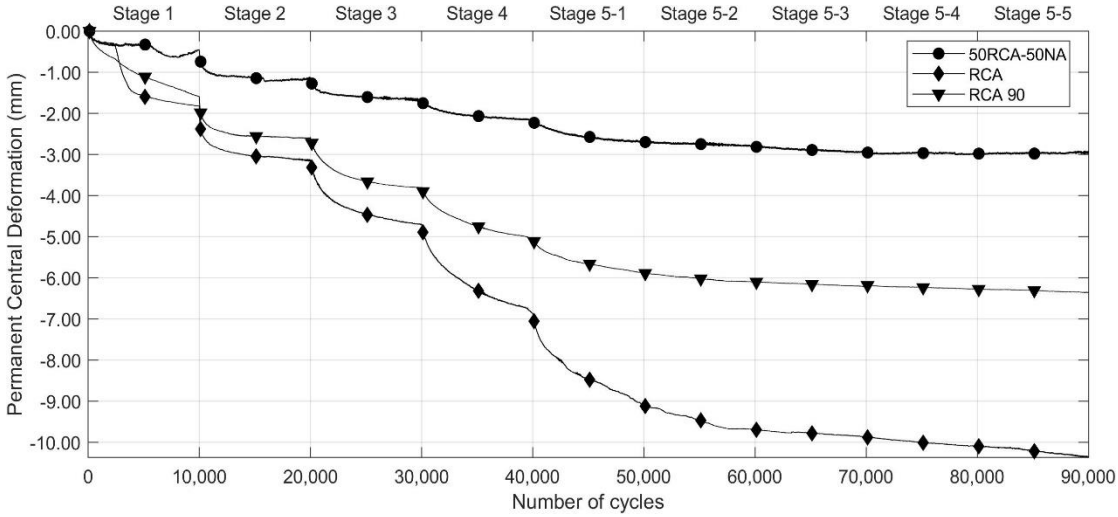

Fig. 11 Surface displacements for RCA and the 50RCA-50NA samples with 60 mm thick base and RCA with 90 mm base

approximately 30,000 cycles. Furthermore, the inclusion of the geogrid significantly enhances rutting resistance, reducing rut depth by 52% after 30,000 loading cycles. By the end of the test, the reinforced RCA sample exhibited a permanent deformation of approximately 4 mm, indicating a 60.8% reduction in deformation due to the geogrid's reinforcing effect. This outcome highlights the effectiveness of geogrid reinforcement in enhancing the durability and long-term stability of RCA-based base materials. As reported by Abu-Farsakh *et al*. (2016) and Aregbesola and Byun (2024), the incorporation of geosynthetic reinforcement results in a redistribution of the applied load over a larger area, effectively minimising stress concentration and promoting a more uniform vertical stress distribution across the subgrade layer. As a result, the subgrade experiences a lower maximum vertical stress and, consequently, resulting in a decrease in permanent vertical strain within the subgrade.

To better understand and compare the improvements induced by the geogrid at each loading stage, the improvement ratio (IR) is calculated using the following equation

$$IR(\%) = \frac{|S_R - S_{UR}|}{S_{UR}} \times 100 \quad (1)$$

where IR is the improvement ratio, S_R is the permanent displacement accumulated within a given number of cycles for the reinforced sample, and S_{UR} is the permanent displacement accumulated at the same number of cycles for the unreinforced sample.

Fig. 13 shows the IRs calculated for both reinforced NA and reinforced RCA samples. The IR was determined at the end of each of the first four loading stages, and for the 550 kPa stress level, the IR was calculated after every 10,000 cycles. The IRs for the first three loading stages of NA were determined, as the unreinforced NA failed at the start of stage 4. It is observed that the geogrid reduces the rutting depth of NA by approximately 60% at each stage. For the RCA sample, the IR value is approximately 50% for the first four stages. It then increases significantly to 90%

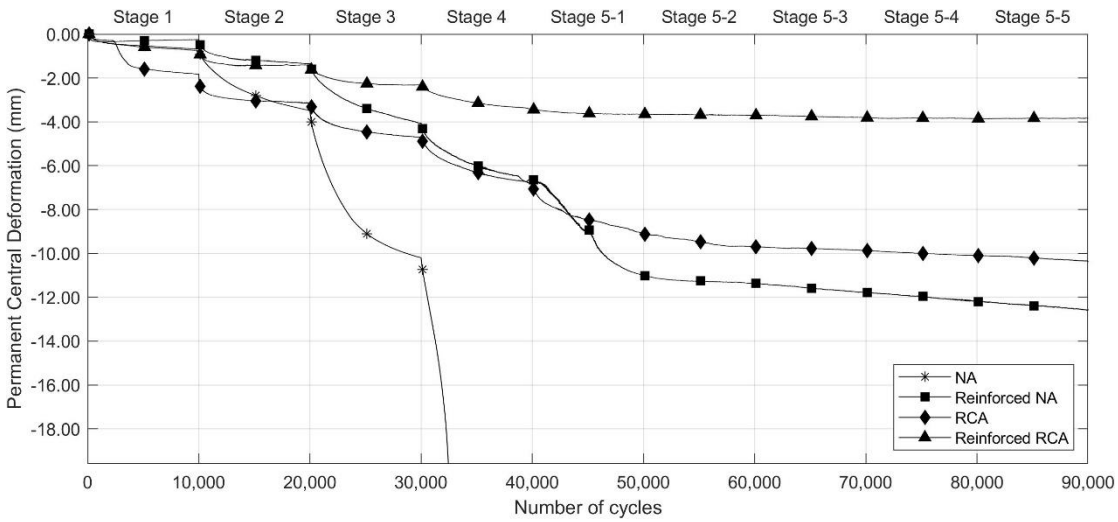

Fig. 12 Surface displacements for unreinforced and reinforced NA and RCA samples

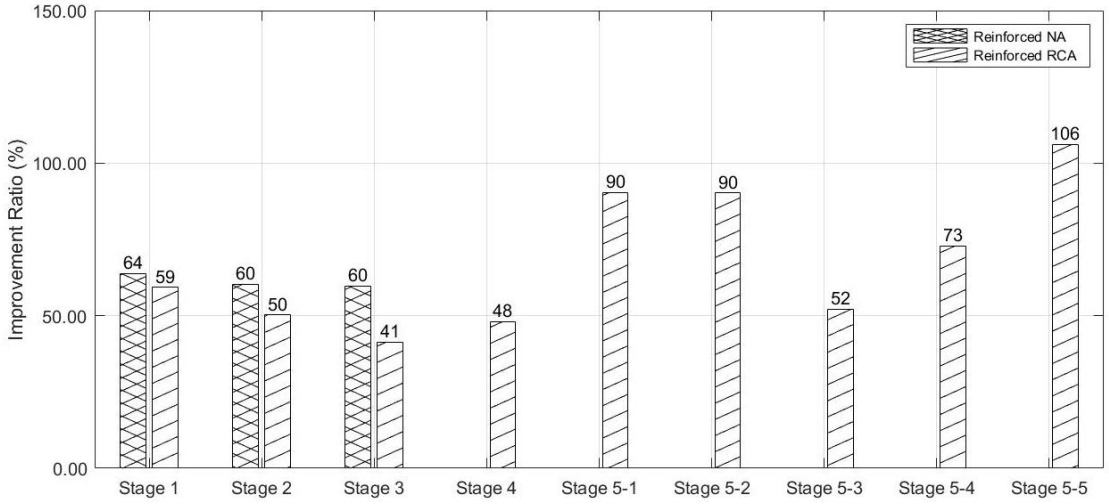

Fig. 13 Improvement ratios for reinforced NA and reinforced RCA samples at each stage

during the first two 10,000 cycles of stage 5, decreases to 50% during the third 10,000 cycles, and shows a significant increase again in the final two 10,000 cycles. As shown in Fig. 12, the permanent deformation of the unreinforced RCA sample exhibits plastic creep behaviour, rapidly accumulating during the first 20,000 cycles of stage 5, with the accumulation rate gradually slowing after 20,000 cycles. After stage 5-3, a sudden rise in the rate of rut depth accumulation is observed during the final two 10,000 cycles. In contrast, the permanent deformation of the reinforced RCA sample shows plastic behaviour, with a significant increase during stage 5-1. Following this, the rate of increase gradually decreases in the subsequent cycles, eventually stabilising and reaching nearly constant values after stage 5-2. Therefore, the variation in IR values shown in Fig. 13 for reinforced RCA is primarily related to the changes in permanent deformation observed in the unreinforced RCA samples. When the unreinforced RCA sample experiences significant permanent deformation, the IR value increases. Conversely, as the rate of permanent deformation accumulation in the unreinforced RCA decreases, the IR value decreases as well. In general, it can be concluded that the geogrid enhances rutting resistance, providing the samples with greater stability.

3.2.4 Surface permanent deformation profiles

The total surface deflection was measured using the loading plunger and four LVDTs positioned 100 mm from the centre of the loading area. Fig. 14 displays the deflection basins for all test samples at the end of each stage, except for the NA sample, which failed at the beginning of stage 4. As expected, with an increase in loading amplitude, the surface of the samples exhibited progressively greater settlement. For each sample, the maximum deflection occurred directly beneath the centre of the loading area, and the magnitude of the deflection diminished with increasing distance from the centre. The reinforced samples consistently showed lower displacement compared to the unreinforced models, indicating that the geogrid was effective in reducing surface settlements. Furthermore, at stages 3 and 4, the NA sample exhibited significant surface heaving prior to failure. As the

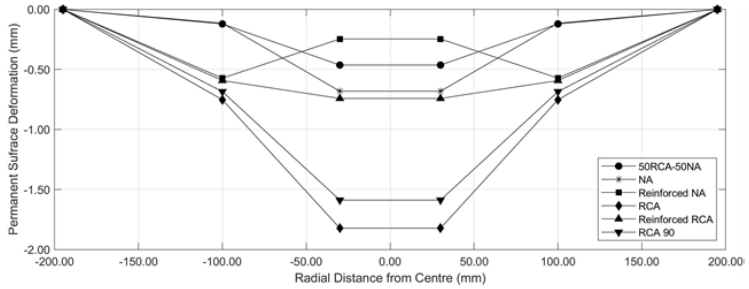

(a) stage 1

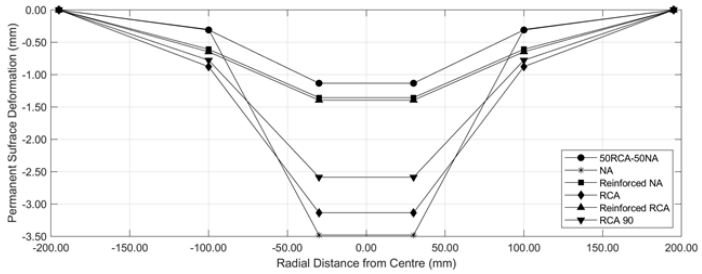

(b) stage 2

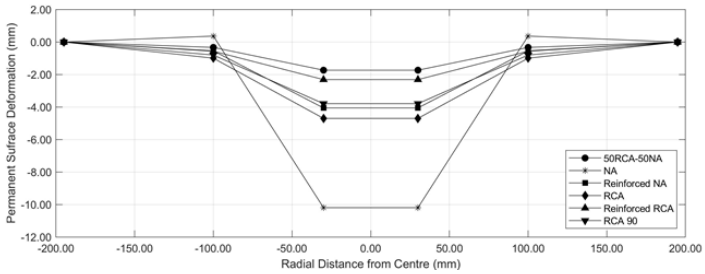

(c) stage 3

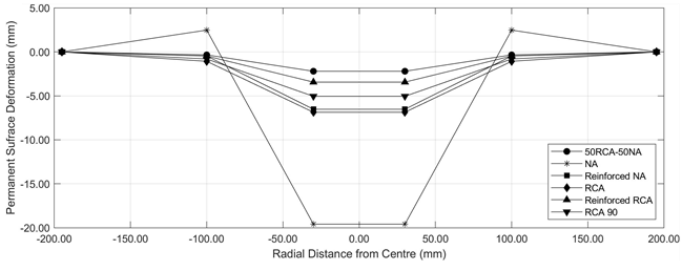

(d) stage 4

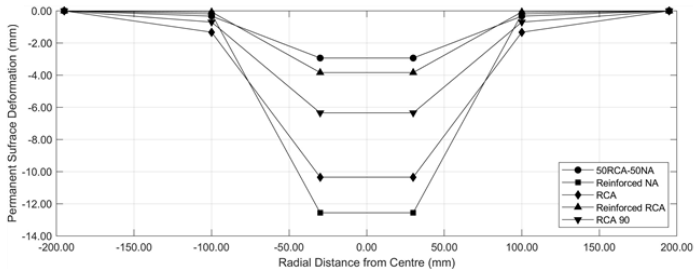

(e) stage 5

Fig. 14 Surface displacements for samples at the end of: (a) stage 1, (b) stage 2, (c) stage 3, (d) stage 4, (e) stage 5

settlement at the loading area became substantially high, it resulted in the upward movement of the surrounding soil, a clear indication of the sample's structural failure.

4. Conclusions

The results show that the RCA material used in this

study has a great quality and can be used as an alternative aggregate for the base layer in road construction. The following conclusions can be drawn:

- The results of CBR tests and RLTTs suggest that incorporating 50% RCA into NA can potentially increase the CBR value and resilient modulus, indicating the potential application of RCA to partially replace NA in road base and subbase materials.
- The permanent deformation versus number of cycles plots obtained from the small-scale cyclic loading tests show that permanent deformation increases with the number of loading cycles. However, the rate of increase in permanent deformation decreases with further increases in the number of cycles. These test results also demonstrate that the 50RCA-50NA mixture has the smallest rutting depth, indicating its greater intrinsic strength.
- The geogrid significantly improves the behaviour of both the NA and RCA samples by reducing permanent deformation and extending service life. It reduces rut depth by 52% after 30,000 loading cycles for the NA sample and by 60.8% for the RCA sample at the end of the test.
- The maximum deflection occurs directly beneath the centre of the loading area, with the magnitude of deflection decreasing as the distance from the centre increases.

While this paper provides valuable insights into the potential use of RCA in road construction, its findings are limited to a single type of geogrid and RCA. The stiffness and aperture size of the geogrid, as well as the type of RCA, may influence the test results. Further research is needed to address their impact. Additionally, conducting a life cycle assessment and life cycle cost analysis would provide a more comprehensive understanding of the environmental and economic impacts of RCA application. Moreover, the relationship between laboratory cyclic loading test results and pavement behaviour under field conditions can be established through numerical simulations, which the authors are currently conducting.

Acknowledgments

The authors would like to acknowledge the financial support from the Australian Research Council Linkage Project (ARC-LP220100186). The financial and technical assistance from industry partners, including Australian Road Research Board (ARRB), Global Synthetics Pty Ltd, FSG Geotechnics & Foundations, and ACT Geotechnical Engineers Pty Ltd, is greatly acknowledged. The authors also wish to thank the technical staff from the School of Engineering and Technology at the University of New South Wales, Canberra, especially Jim Baxter and Umesh Kaini, for their valuable assistance in the experimental work presented in this paper.

References

AASHTO T307. (2017), Standard Method of Test for Determining the Resilient Modulus of Soils and Aggregate Materials. American Association of state Highway and Transportation Officials, Washington, DC, AASHTO T307.

Abu-Farsakh, M., Hanandeh, S., Mohammad, L. and Chen, Q. (2016), "Performance of geosynthetic reinforced/stabilized paved roads built over soft soil under cyclic plate loads", *Geotex. Geomembranes*, **44**, 845-853. https://doi.org/10.1016/j.geotexmem.2016.06.009.

Alnedawi, A. and Rahman, M.A. (2021), "Recycled concrete aggregate as alternative pavement materials: Experimental and parametric study", *J. Transport. Eng. Part B: Pavements*, **147**, 04020076. https://doi.org/10.1061/JPEODX.0000231.

Al-Swaidani, A.M., Meziab, A., Khwies, W.T., Al-Bali, M. and Lala, T. (2024), "Building MLR, ANN and FL models to predict the strength of problematic clayey soil stabilized with a combination of nano lime and nano pozzolan of natural sources for pavement construction", *Int. J. Geo-Eng.*, **15**(1),.2. https://doi.org/10.1186/s40703-023-00201-1.

Aregbesola, S.O. and Byun, YH. (2024), "Classification of geogrid reinforcement in aggregate using machine learning techniques", *Int. J. Geo-Eng.*, **15**(1), .4. https://doi.org/10.1186/s40703-024-00206-4.

Arm, M. (2001), "Self-cementing properties of crushed demolished concrete in unbound layers: results from triaxial tests and field tests", *Waste Management*, **21**, 235-239. https://doi.org/10.1016/S0956-053X(00)00095-7.

Arulrajah, A., Disfani, M.M., Horpibulsuk, S., Suksiripattanapong, C. and Prongmanee, N. (2014), "Physical properties and shear strength responses of recycled construction and demolition materials in unbound pavement base/subbase applications", *Constr. Build. Mater.*, **58**, 245-257. https://doi.org/10.1016/j.conbuildmat.2014.02.025.

Arulrajah, A., Piratheepan, J., Ali, M. and Bo, M. (2012), "Geotechnical properties of recycled concrete aggregate in pavement sub-base applications", *Geotech. Test. J.*, **35**, 743-751. https://doi.org/10.1520/GTJ103402.

ASTM-D698. (2021), Standard Test Methods for Laboratory Compaction Characteristics of Soil Using Standard Effort (12,400 ft-lbf/ft^3 (600 kN-m/m^3)).

ASTM-D1883. (2021), Standard test method for California bearing ratio (CBR) of laboratorycompacted soils.

ASTM-D4318. (2018), Standard Test Methods for Liquid Limit, Plastic Limit, and Plasticity Index of Soils.

Azam, A. and Cameron, D. (2013), "Geotechnical properties of blends of recycled clay masonry and recycled concrete aggregates in unbound pavement construction", *J. Mater. Civil Eng.*, **25**, 788-798. https://doi.org/10.1061/(ASCE)MT.1943-5533.0000634.

Boussinesq, J. and Caquot, M.A. (1885), "Application des potentiels: à l'étude de l'équilibre et du mouvement des solides élastiques. Albert Blanchard, Paris, France (in French.)", [Reprinted, 1969 with an introduction by A. Caquot, Gauthier-Villars, Paris.]

Chummar, A. (1972), "Bearing capacity theory from experimental results", *J. Soil Mech. Found. Division*, **98**, 1311-1324. https://doi.org/10.1061/JSFEAQ.0001816.

Department of Transport and Main Roads. (2022), [Online]. Department of Transport and Main Roads website, Queensland Government Available: https://www.tmr.qld.gov.au (Accessed 23 October 2024).

Gabr, A. and Cameron, D. (2012), "Properties of recycled concrete aggregate for unbound pavement construction", *J. Mater. Civil Eng.*, **24**, 754-764. https://doi.org/10.1061/(ASCE)MT.1943-5533.0000447.

Gabr, A., Mills, K. and Cameron, D. (2013), "Repeated load triaxial testing of recycled concrete aggregate for pavement base construction", *Geotech. Geol. Eng.*, **31**, 119-132. https://doi.org/10.1007/s10706-012-9572-8.

Gómez-Soberón, J.M. (2002), "Porosity of recycled concrete with substitution of recycled concrete aggregate: An experimental study", *Cement Concrete Res.*, **32**, 1301-1311. https://doi.org/10.1016/S0008-8846(02)00795-0.

Gu, F., Sahin, H., Luo, X., Luo, R. and Lytton, R.L. (2015), "Estimation of resilient modulus of unbound aggregates using performance-related base course properties", *J. Mater. Civil Eng.*, **27,** 04014188. https://doi.org/10.1061/(ASCE)MT.1943-5533.0001147.

Katz, A. (2003), "Properties of concrete made with recycled aggregate from partially hydrated old concrete", *Cement Concrete Res.*, **33,** 703-711. https://doi.org/10.1016/S0008-8846(02)01033-5.

Lee, J. and Salgado, R. (2005), "Estimation of bearing capacity of circular footings on sands based on cone penetration test", *J. Geotech. Geoenviron. Eng.*, **131,** 442-452. https://doi.org/10.1061/(ASCE)1090-0241(2005)131:4(442).

Nam, B.H., An, J. and Curate, T. (2023), "Effect of reaction temperature and time on the formation of calcite precipitation of recycled concrete aggregate (RCA) for drainage applications", *Geomech. Eng.*, **33**(1), 65-75. https://doi.org/10.12989/gae.2023.33.1.065.

NWR. (2022), National Waste Report. Canberra, Australia: Department of Agriculture, Water and the Environment. (Accessed 24 October 2024).

Sagoe-Crentsil, K.K., Brown, T. and Taylor, A.H. (2001), "Performance of concrete made with commercially produced coarse recycled concrete aggregate", *Cement Concrete Res.*, **31**, 707-712. https://doi.org/10.1016/S0008-8846(00)00476-2.

Ok, B., Colakoglu, H. and Dagli, U. (2023), "Evaluation of the geogrid-various sustainable geomaterials interaction by direct shear tests", *Geomech. Eng.*, **34**(2), 173-186. https://doi.org/10.12989/gae.2023.34.2.173.

Thai, H.N., Nguyen, T.D., Nguyen, V.T., Nguyen, H.G. and Kawamoto, K. (2022), "Characterization of compaction and CBR properties of recycled concrete aggregates for unbound road base and subbase materials in Vietnam", *J. Mater. Cycles Waste Management,* 1-15. https://doi.org/10.1007/s10163-021-01333-1.

Toka, E.B. and Olgun, M. (2022), "Performance of granular road base and sub-base layers containing recycled concrete aggregate in different ratios", *Int. J. Pavement Eng.*, **23**, 3729-3742. https://doi.org/10.1080/10298436.2021.1916819.

Van Dam, T.J., Harvey, J., Muench, S.T., Smith, K.D., Snyder, M.B., Al-Qadi, I.L., Ozer, H., Meijer, J., Ram, P. and Roesler, J. R. (2015), Towards sustainable pavement systems: a reference document. United States. Federal Highway Administration.

Vicroads. (2011), Section 820: Crushed concrete for pavement subbase and light duty base. https://webapps.vicroads.vic.gov.au (Accessed 24 October 2024).

Wang, C., Chazallon, C., Hornych, P. and Braymand, S. (2023), "Permanent and resilient deformation behaviour of recycled concrete aggregates from different sources, in pavement base and subbase", *Road Mater. Pavement Design*, **24**, 2245-2262. https://doi.org/10.1080/14680629.2022.2134048.

Xiao, J., Li, J. and Zhang, C. (2005), "Mechanical properties of recycled aggregate concrete under uniaxial loading", *Cement Concrete Res.*, **35**, 1187-1194. https://doi.org/10.1016/j.cemconres.2004.09.020.